



**HAL**  
open science

## **Experimental fatigue behavior of carbon/flax hybrid composites under tensile loading**

Mariam Ben Ameer, Abderrahim El Mahi, Jean-Luc Rebiere, Moez Beyaoui,  
Moez Abdennadher, Mohamed Haddar

► **To cite this version:**

Mariam Ben Ameer, Abderrahim El Mahi, Jean-Luc Rebiere, Moez Beyaoui, Moez Abdennadher, et al.. Experimental fatigue behavior of carbon/flax hybrid composites under tensile loading. *Journal of Composite Materials*, 2020, 55 (5), pp.002199832095490. 10.1177/0021998320954903 . hal-02954676

**HAL Id: hal-02954676**

**<https://hal.science/hal-02954676>**

Submitted on 14 Mar 2024

**HAL** is a multi-disciplinary open access archive for the deposit and dissemination of scientific research documents, whether they are published or not. The documents may come from teaching and research institutions in France or abroad, or from public or private research centers.

L'archive ouverte pluridisciplinaire **HAL**, est destinée au dépôt et à la diffusion de documents scientifiques de niveau recherche, publiés ou non, émanant des établissements d'enseignement et de recherche français ou étrangers, des laboratoires publics ou privés.

# Experimental fatigue behavior of carbon/flax hybrid composites under tensile loading

Mariem Ben Ameer<sup>1,2</sup>, Abderrahim El Mahi<sup>1</sup>,  
Jean-Luc Rebiere<sup>1</sup>, Moez Beyaoui<sup>2</sup>, Moez Abdennadher<sup>2</sup> and Mohamed Haddar<sup>2</sup>

## Abstract

The aim of the present study is to investigate the mechanical behavior of carbon/flax hybrid composites under static and fatigue tensile loading. The failure characteristics and parameters used in the fatigue tests were deduced from the static ones. The effect of the applied stress level, hybridization and stacking sequences on the stiffness, hysteresis loops, dissipated energy and damping, were studied for a various number of cycles during fatigue tests. The Wohler S-N curves were constructed to investigate the effect of hybridization on the fatigue behavior. The results obtained show that the fatigue performance as well as the fatigue resistance increase with the increase of the volume fraction of carbon fiber. Nevertheless, the damping ratio and the fatigue life increase with the increase of the flax fiber volume fraction.

## Keywords

Carbon fibers, flax fibers, hybrid composites, fatigue, life prediction

## Introduction

In the last decades, composites reinforced with natural fibers (such as hemp, kenaf, flax, etc. . .) have been extensively used by many researchers to face current engineering challenges.<sup>1,2</sup> Bio-based composites are ecological, biodegradable and they have unlimited availability.<sup>3</sup> In addition, plant fibers can be an alternative to conventional ones such as carbon, glass and aramid because they present numerous advantages. In fact, they have relatively interesting specific properties.<sup>4,5</sup>

Moreover, owing to the good properties of composites reinforced with flax fibers, they are the most interesting plant fiber-based composites that have been studied.<sup>6-8</sup> Monti et al.,<sup>9</sup> Haggui et al.<sup>10</sup> and Hughes et al.<sup>11</sup> studied the mechanical behavior of unidirectional flax fiber reinforced composites. Additionally, vibrational behavior has become an important factor for high performance applications. Indeed, Monti et al.<sup>12</sup> evaluated the damping properties of the composites reinforced with flax fibers. Duc et al.<sup>13</sup> experimentally studied the mechanical and vibrational behavior of flax, glass and carbon fiber composites. They found that composites reinforced with carbon

fibers have higher performance for mechanical properties, but poor vibrational behavior compared to glass and carbon fiber composites.

In order to improve the dynamic properties of carbon fiber composites, recent studies have proposed the development of hybrid composites with carbon and flax fibers.<sup>14</sup> Reversely, by hybridization of flax fibers with carbon ones, the property of variability and moisture sensitivity of natural fibers can be reduced.<sup>15,16</sup> Consequently, they can be suitable for high performance structural use. Recently, hybrid composites have been used on industrial applications such as manufacturing of racing sailboats (Huntsman), tennis rackets (Artengo) and skis (Down skis). Assarar et al.<sup>17</sup> and Ben Ameer et al.<sup>18</sup> evaluated the vibrational

---

<sup>1</sup>Acoustics Laboratory, Le Mans University (LAUM), France

<sup>2</sup>Laboratory of Mechanics, Modeling and Production (LA2MP), National School of Engineers of Sfax, University of Sfax, Tunisia

## Corresponding author:

Mariem Ben Ameer, Le Mans Université, Av. O. Messiaen 72085 Le Mans Cedex 9, France, Le Mans 72085, France.

Email: Mariem.Ben\_Ameer.Etu@univ-lemans.fr

behavior of hybrid carbon-flax fiber composites. They found that damping properties of carbon fiber composites were improved by hybridization with flax fibers. Flynn et al.<sup>19</sup> and Fiore et al.<sup>20</sup> studied the quasi-static mechanical behavior of carbon-flax hybrid composites.

In addition to the quasi-static mechanical behavior, the cyclic fatigue behavior of composites is of great importance since they are subjected to cyclic loading in a variety of applications. Furthermore, the behavior of the fibers themselves can affect the fatigue behavior of the composite. The tensile fatigue behavior of individual sisal fibers has been investigated by many authors.<sup>21,22</sup> For monitoring the damage, Towo and Ansel<sup>23</sup> used cyclic hysteresis in order to evaluate the loss of stiffness, material energy dissipation and damage development. Liang et al.<sup>24</sup> investigated the mechanical behavior of glass and flax fiber composites through static and fatigue tensile tests. They found that the fatigue resistance of flax fiber composites is lower than that of glass fiber composites. They attributed this fact to the difference in their ultimate tensile strength. Shah et al.<sup>25</sup> examined the fatigue life of aligned plant fiber composites. They found that even though the fatigue performance of glass fiber composites is notably superior to plant fiber composites, the fatigue strength degradation rates of plant fiber composites are the lowest. El Sawi et al.<sup>26</sup> investigated the fatigue performance of flax-fiber reinforced composites. They used infrared thermography for predicting the fatigue life. They showed that there is a correlation between the residual strain increase and the matrix cracking density. Mahboob and Bougherara<sup>27</sup> carried out a review on the response of natural fiber composites under cyclic loading. Gassan<sup>28</sup> evaluated the tension-tension fatigue behavior of composite materials made of jute and flax yarns and woven as reinforcement for polyester, epoxy and polypropylene resin. He found that fiber type/properties, textile architecture and fiber content have an effect on the fatigue behavior. The results obtained were also found by Bensadoun et al.<sup>29</sup> Zhang and Hartwig<sup>30</sup> investigated the damage processes of unidirectional carbon and glass fiber composites by cyclic fatigue loading. They found that the damping is more sensitive than stiffness, that's why it is recommended for the evaluation of the damage processes induced by fatigue tests.

The present paper focuses on the investigation of the mechanical behavior of relatively new materials: carbon/flax hybrid fibers reinforced epoxy composites with different fibers content and different stacking sequences. The fatigue performance of this type of materials have not been deeply studied yet. The non-hybrid and hybrid laminates were subjected to static and fatigue tensile loading. The fatigue tests were carried out for different loading levels from 0.6 to 0.85 of

the average monotonic ultimate tensile stress (UTS). First, the effect of the loading level on the stiffness, hysteresis loops, dissipated energy and loss factor was studied for various numbers of cycles during cyclic fatigue tests. After that, a comparison was conducted between the different stacking sequences materials for a given applied stress level to study the effect of the hybridization up to a common number of cycles. Finally, an investigation of the fatigue performance through the Wohler lifetime diagrams on composites, cyclic loading behavior was made.

## Materials and experimental procedure

### Materials and manufacturing

The unidirectional carbon fiber reinforced epoxy ( $[C_3]_s$ ), flax fiber reinforced epoxy ( $[F_3]_s$ ) and hybrid fiber reinforced epoxy laminates considered in this work were made from commercial dry rolls of carbon fabrics and flax tape, with a mass density of 300 g/m<sup>2</sup> and 200 g/m<sup>2</sup>, respectively. Four hybrid fiber composites were proposed with different stacking sequences ( $[C_2/F]_s$ ,  $[C/F_2]_s$ ,  $[F/C_2]_s$  and  $[F_2/C]_s$ ) which are presented in Figure 1. The unidirectional carbon and flax fibers were furnished by Sicomin and Lineo,<sup>31</sup> respectively. The matrix type was an epoxy system based on SR 1500 resin with SD 2505 hardener furnished by Sicomin. Fiber plies were first cut from the roll. The carbon fibers were used as received. However, the flax fibers were dried in an oven at 110 °C for one hour to enhance their mechanical properties as found by Baley et al.<sup>32</sup> Composite plates were elaborated by using a manual lay-up method with the resin matrix. They consist of six layers all oriented in the longitudinal direction of the reinforcement. They were cured at room temperature (20 °C) at pressure of 0.5 bar with a vacuum molding technique for 7 hours. The samples using flax fibers were dried enough, it was provided by a research work of Malloum et al.<sup>33</sup> In fact, after demolding, they were kept at room temperature for one or two weeks in order to obtain complete polymerization of the resin. Finally, the test specimens have been cut up using a diamond band saw. The thickness, fiber volume fraction and density of the non-hybrid and hybrid laminates are presented in Table 1.

### Experimental setup

Experimental static and fatigue tensile tests were carried out on a standard hydraulic machine (INSTRON 8516) with a 100 kN load cell. A dedicated personal computer was interfaced to the machine for monitoring and data acquisition. The strains in the tensile direction were measured by means of an extensometer.

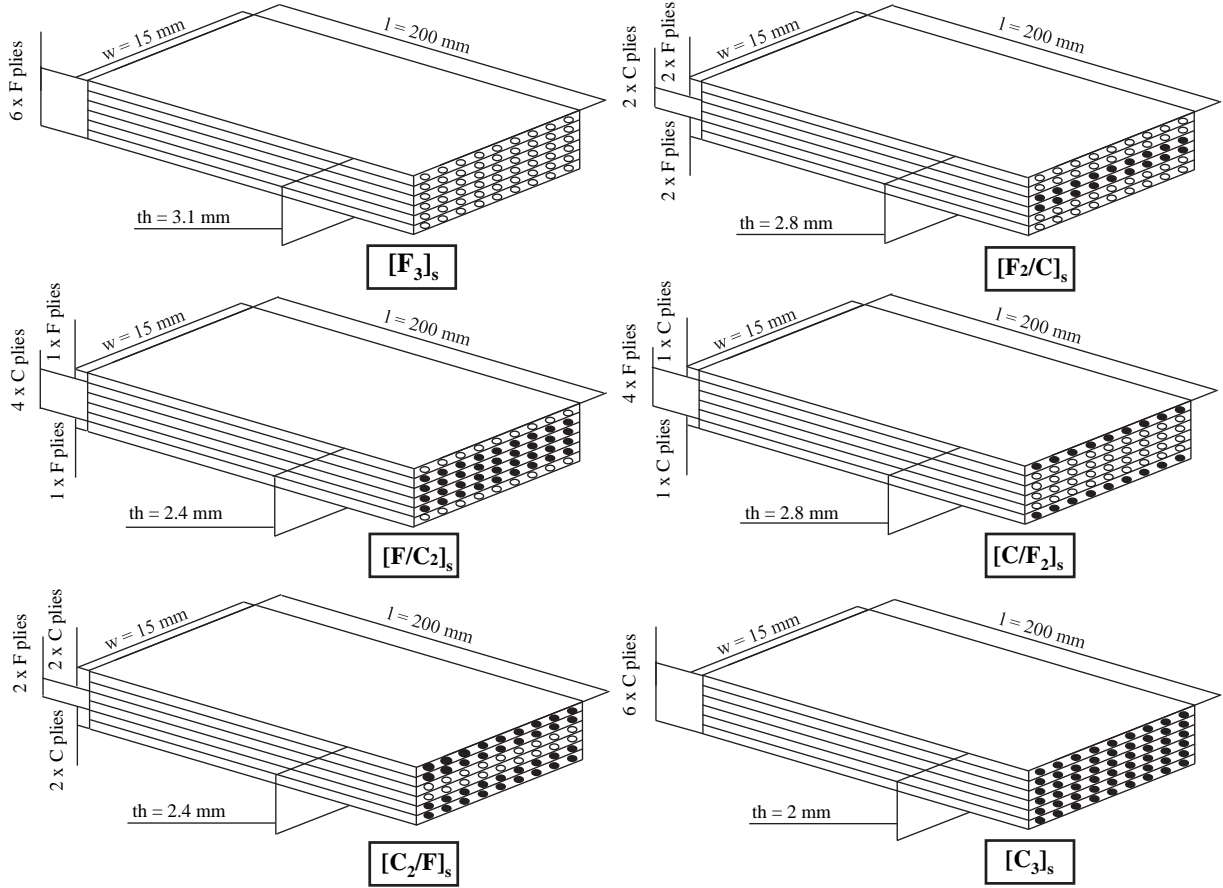


**Figure 1.** Schematic illustration of the six studied stacking sequences.

**Table 1.** Thickness, fiber volume fraction and density of non-hybrid and hybrid laminates.

Stacking sequences	Nominal thickness th (mm)	Fibre volume fraction $V_f$ (flax/carbon)	Density ( $\text{kg/m}^3$ )
$[F_3]_s$	3.10	0.32/0.00	1140
$[F_2/C]_s$	2.80	0.22/0.19	1181
$[F/C_2]_s$	2.40	0.12/0.37	1266
$[C/F_2]_s$	2.80	0.22/0.19	1175
$[C_2/F]_s$	2.40	0.12/0.37	1234
$[C_3]_s$	2.00	0.00/0.55	1340

The specimens were tested according to the standard test method ASTM D3039/D3039 M.<sup>34</sup> The geometry of static and fatigue samples was similar as presented in Figure 1. The samples having a constant rectangular cross section and without tabs are mounted in the grips of the mechanical testing machine with a clamping length of 50 mm. Three to five specimens were tested statically to failure to determine the ultimate

strength UTS of each type of specimen. Specimens were loaded at a cross-head speed of 1 mm/min. The tests were performed at room temperature.

The fatigue tests were conducted using a sinusoidal type of waveform at a constant frequency rate of 10 Hz. The tests were performed under load amplitude control. The applied stress level  $r$  was varied from 0.6 to 0.85, where  $r = \sigma_{\max}/\text{UTS}$  with  $\sigma_{\max}$  is the maximum stress applied. Five fatigue loading levels were considered:  $r = 0.6, 0.65, 0.75, 0.8$  and  $0.85$ . Figure 2 shows an example of load waveform used during the fatigue tests. The specimens were tested in tension-tension mode with an applied stress ratio  $R = \sigma_{\min}/\sigma_{\max}$  maintained constant and equal to 0.1, where  $\sigma_{\min}$  is the minimum stress applied. For each fatigue testing level, at least five samples were tested to failure. First the specimen was loaded at a constant tensile rate of 1 mm/min, where the applied load increases until reaching the mean applied stress  $\sigma_{\text{mean}}$  where  $\sigma_{\text{mean}} = (\sigma_{\max} + \sigma_{\min})/2$ . Then, the specimen was loaded up to failure with a sinusoidal waveform characterized by the amplitude  $\sigma_{\text{amp}}$  where  $\sigma_{\text{amp}} = (\sigma_{\max} - \sigma_{\min})/2$ .

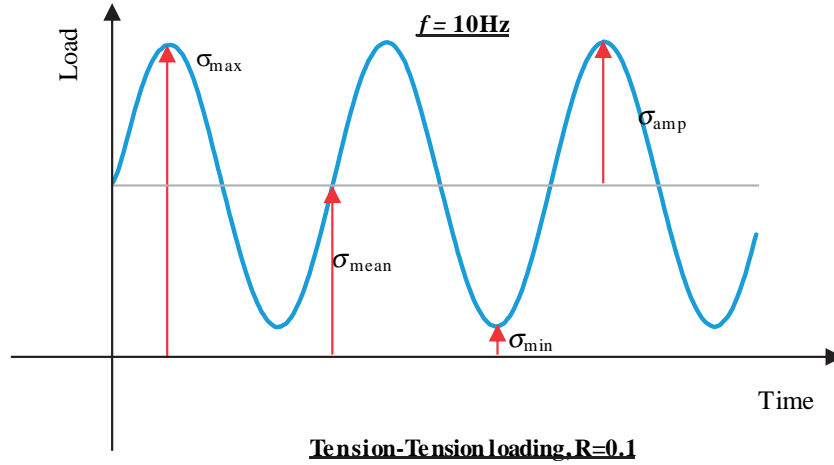


**Figure 2.** Typical load-time curves under fatigue loading test.

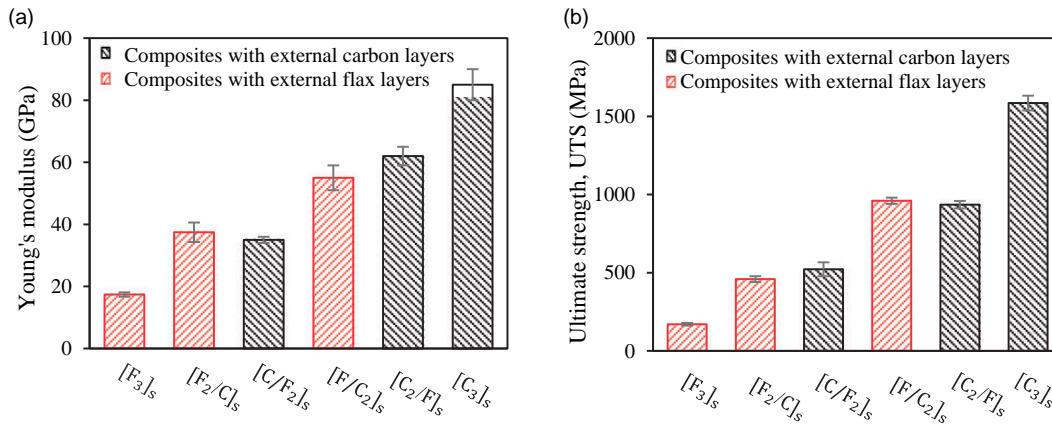


**Figure 3.** Evolution of the mechanical properties of flax/carbon hybrid composites: (a) Young's modulus and (b) ultimate strength.

**Table 2.** Mechanical properties of flax, carbon and hybrid fiber composites, standard deviations in brackets.

Stacking sequences	[F <sub>3</sub> ] <sub>s</sub>	[F <sub>2</sub> /C] <sub>s</sub>	[F/C <sub>2</sub> ] <sub>s</sub>	[C/F <sub>2</sub> ] <sub>s</sub>	[C <sub>2</sub> /F] <sub>s</sub>	[C <sub>3</sub> ] <sub>s</sub>
Young's modulus (GPa)	17.4 (0.7)	37.5 (3.1)	55.0 (5.0)	35.0 (1.0)	62.0 (3.0)	85.0 (5.0)
Ultimate strength, UTS (MPa)	170 (8.3)	460 (18.5)	960 (7.0)	522 (44.5)	935 (24.0)	1585 (47.0)
Failure load, $F_u$ (kN)	7.8 (1.1)	21.7 (1.1)	38 (0.7)	23.4 (1.5)	36.5 (1)	54.6 (1.5)

### Static mechanical behavior

The experimental monotonic tensile tests were performed on specimens of non-hybrid and hybrid carbon/flax fiber with different stacking sequences. The average ultimate tensile strength and modulus derived from recorded data for all types of laminated composites are illustrated in Figure 3. These results show that when the carbon fiber volume fraction increases, the composite exhibit a high performance for the ultimate tensile strength and the Young modulus. Also, it is readily observed that the mechanical

properties of hybrid laminates, with same volume fraction of fibers but different position of layers, are broadly similar to each other. For all composites, the Young's modulus, the ultimate strength UTS and the failure load  $F_u$  obtained from the tests are presented in Table 2. The ultimate tensile strength UTS of [F<sub>3</sub>]<sub>s</sub> laminate is lower by 85% than that of [C<sub>3</sub>]<sub>s</sub> laminate, where the UTS of [C/F<sub>2</sub>]<sub>s</sub> and [F<sub>2</sub>/C]<sub>s</sub> laminates are lower by around 60% and the UTS of [C<sub>2</sub>/F]<sub>s</sub> and [F/C<sub>2</sub>]<sub>s</sub> laminates are only lower by around 30% than that of [C<sub>3</sub>]<sub>s</sub> laminate. In Table 2, it should be emphasized that the differences in properties are due, not to stacking

sequences, but to various fiber volume fractions. This result was obtained owing to the higher intrinsic mechanical properties of carbon fibers in comparison with flax fibers. In the next part, the performance of all stacking sequences under cyclic fatigue loading is studied.

## Fatigue results of non-hybrid and hybrid carbon/flax epoxy composites

### Stiffness degradation

Carbon fiber composites, flax fiber composites and hybrid fiber composites were tested under cyclic fatigue loading at different applied stress levels up to failure. To follow the progression of damage by fatigue of these composites, the evolution of the stiffness constitutes one of the most used methods.<sup>35,36</sup> Generally, the stiffness loss is characterized by the evolution of the maximum displacement  $d_{\max}$  related to that obtained in the first cycle  $d_{0\max}$  ( $d_{0\max}/d_{\max}$ ). During the tests carried out, we recorded the evolution of the maximum displacement  $d_{\max}$  as a function of the cycle number  $N$ . Each point presented in all figures was the mean values of multiple samples. Figure 4 gives a typical result of the stiffness loss as a function of the cycle number  $N$  for the  $[F_3]_s$  laminate with a loading level  $r=0.6$  in both linear and semi-logarithmic scales. The typical result obtained shows that the loss of the stiffness until the rupture of the test specimens takes place in three distinct phases. At initial phase, a rapid loss of stiffness is recorded from the first cycles which corresponds to the initiation and multiplication of matrix cracking. In the second phase, the stiffness degradation becomes very slow and substantially linear as a function of the cycle number. It corresponds to the stable propagation of matrix cracking, emergence and propagation of delamination and interfacial debonding. The almost of the

life of the specimen is under this phase for approximately 80% of the lifetime with a degradation of rigidity between (10 to 35%). Finally, in the third phase, we record a very short duration of stiffness degradation, consisting of a sudden growth of all types of fatigue damage mechanisms until the breakage of fibers, resulting in the final ruin of the specimen.

The evolution of the stiffness versus the number of cycles ( $N$ ) of the different stacking sequences under different loading levels  $r$  (0.6, 0.65, 0.75, 0.8 and 0.85) using a semi-logarithmic scale are shown in Figure 5. The degree of the damage is highly sensitive to the applied loading level. In fact, the fatigue life increases with the decrease of the applied stress level  $r$  for the different composite materials (Figure 5). As consequence, for a small applied stress ( $r=0.6$ ), corresponding to a small amplitude, a lot of damage mechanisms are activated with a slow propagation, so that the fatigue life is very long. For Figure 5(f), in many cases a rapid drop is shown at the end but in others such as in Figure 5(d), this is absent in the case of  $r=0.6$ . These results are obtained because for carbon composites the rupture is brutal due to its high rigidity. Or, for the other composites, the rapid drop is absent because we have the presence of the flax fibers in the composites.

Figure 6 presents a comparative study of carbon fiber laminate, flax fiber laminate and hybrid fiber laminates for two applied stress levels  $r$  (0.65 and 0.80). The analysis of these results shows that the rates of the stiffness degradation in flax laminates and hybrid laminates for the same applied level are superior than in carbon laminates. At the same applied load level, the fatigue life in flax fiber laminate is superior than that of carbon fiber laminate. For the carbon laminates, the initial damage is small with a considerably high growth rate leading to a very short fatigue life; the total rupture is quickly reached. Moreover, for the

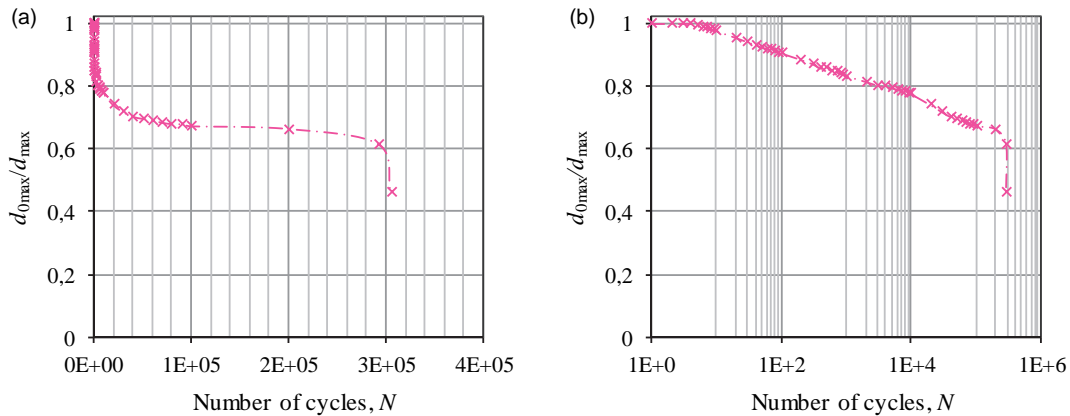


**Figure 4.** A typical curve of the stiffness loss ( $d_{0\max}/d_{\max}$ ) as a function of the cycles number ( $N$ ): (a) linear scale and (b) semi-logarithmic scale.

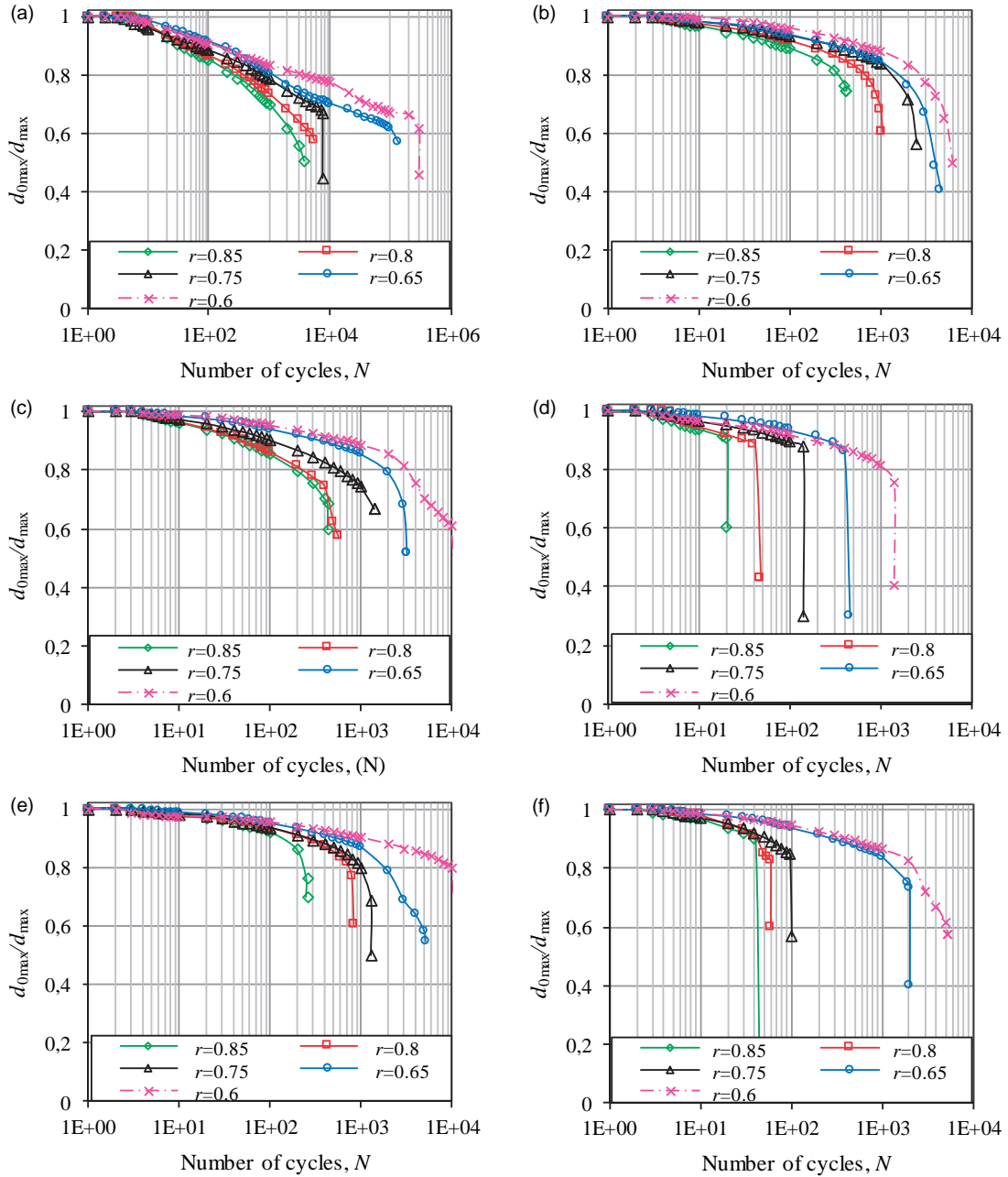


**Figure 5.** Stiffness loss ( $d_{0max}/d_{max}$ ) according to the cycles number for different applied stress levels ( $r$ ) of the different stacking sequences: (a)  $[F_3]_s$ , (b)  $[F_2/C]_s$ , (c)  $[F/C_2]_s$ , (d)  $[C/F_2]_s$ , (e)  $[C_2/F]_s$  and (f)  $[C_3]_s$ .

flax fiber composites and as observed by Mahboob and Bougherara<sup>27</sup> and Bensadoun et al.,<sup>29</sup> they present a longer fatigue life under constant load amplitude cycling. The brutal rupture of carbon fiber laminates occurs after a weak reduction in stiffness, whereas in the case of flax fiber laminate the rupture is less brutal. The presence of flax fiber in the laminate is the cause of a non-linear behavior and a less brittle rupture. The fatigue life of flax laminates is one hundred times greater than that of carbon laminates for an applied load level of  $r=0.65$ . It is observed that carbon laminates

have a better resistance to the stiffness degradation whereas the flax laminates have a better resistance to the fatigue life.

### Hysteresis curves

In order to identify the initiation and the evolution of damage on a specimen under fatigue tests, inspection of the hysteresis curves at different numbers of cycles was carried out. In fact, during cyclic fatigue tests, 100 experimental points were recorded for each cycle.

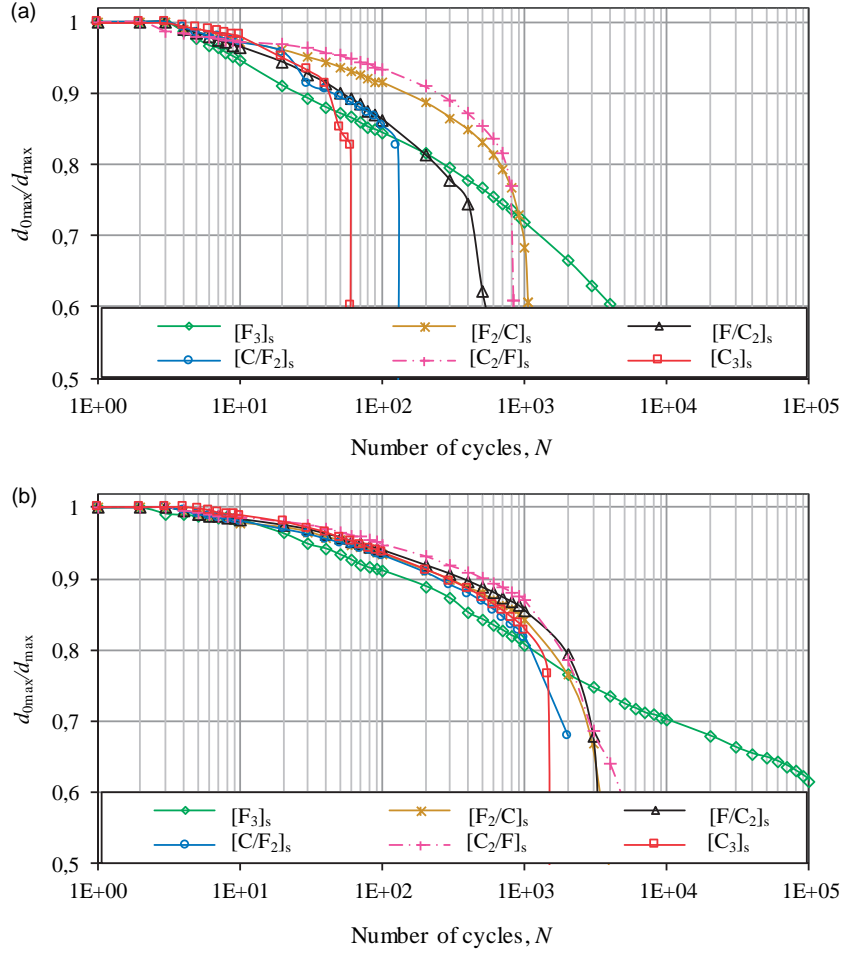


**Figure 6.** Comparative study of Stiffness loss ( $d_{0max}/d_{max}$ ) according to the cycle number ( $N$ ) for two applied stress levels: (a)  $r=0.8$  and (b)  $r=0.65$ .

The load-displacement data was collected in real time. At the applied load level  $r=0.65$ , typical load-displacement loops for loading and unloading cycles at 1, 10,  $10^2$ ,  $10^3$ ,  $10^4$ ,  $10^5$  and the failure cycle ( $1.3 \cdot 10^5$ ) for flax fiber composites and at 1, 10,  $10^2$ ,  $10^3$  and the failure cycle ( $2 \cdot 10^3$ ) for carbon fiber composites are presented in Figure 7. In order to better clarify these figures, the loop of each cycle is translated along the displacement axis. For both non-hybrid composites, the behavior is quite similar. At a constant stress level, it can be seen that the curves of loading and unloading cycles move towards high strains. In fact, maximum displacement increases with the increase of the number of fatigue cycle. It can be seen that hysteresis loops in the first cycle have a large area in loading and unloading for the two composite materials. This fact can be attributed to the high effort needed to the initiation of damage at the beginning of the fatigue test. The area under the hysteresis loops decreases as the number of cycles increases due to the damage development and propagation in the

constituents of composites. During the final cycles, the area of the hysteresis loops tends to increase due to final damage.

The hysteresis cycles are obtained from the curves of loading and unloading versus displacement.

Figures 8 and 9 present a comparison of the hysteresis loops at  $10^0$ ,  $10^1$ ,  $10^2$  and  $10^3$  cycles at applied stress level  $r=0.65$  for specimens with external carbon layers and internal carbon layers, respectively. For all laminates, the behavior is similar whereas the peak loads of hysteresis curves are different. In fact, for each material, we have an ultimate load which is different from the other materials. For any given type of specimen, the hysteresis loops move towards higher strains at a constant stress level. Displacement corresponding to the minimum and maximum loading of loops increases with the number of cycles. Also, it is clearly observed from these hysteresis loops that the strain increases with the increase in the carbon fiber volume fraction which is in accordance with the static strain of samples (Figure 3).



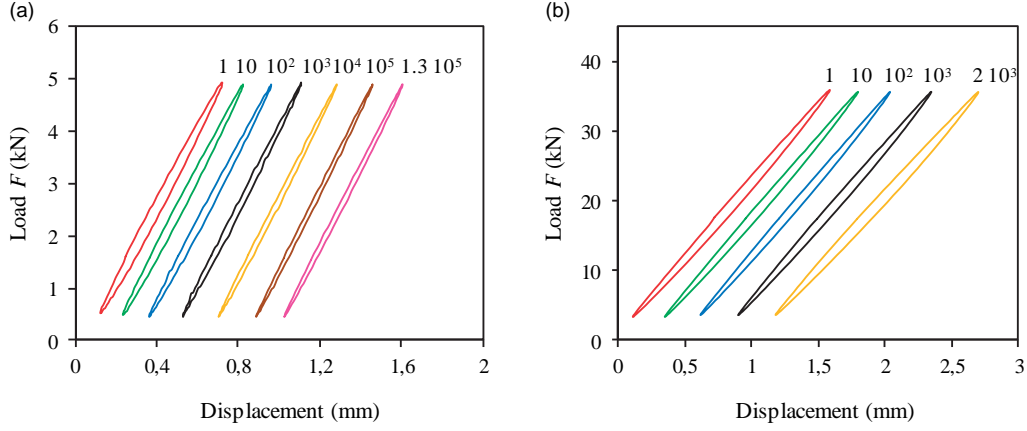


**Figure 7.** Hysteresis curves at the applied load level  $r = 0.65$  a) flax fiber composites and b) carbon fiber composites.

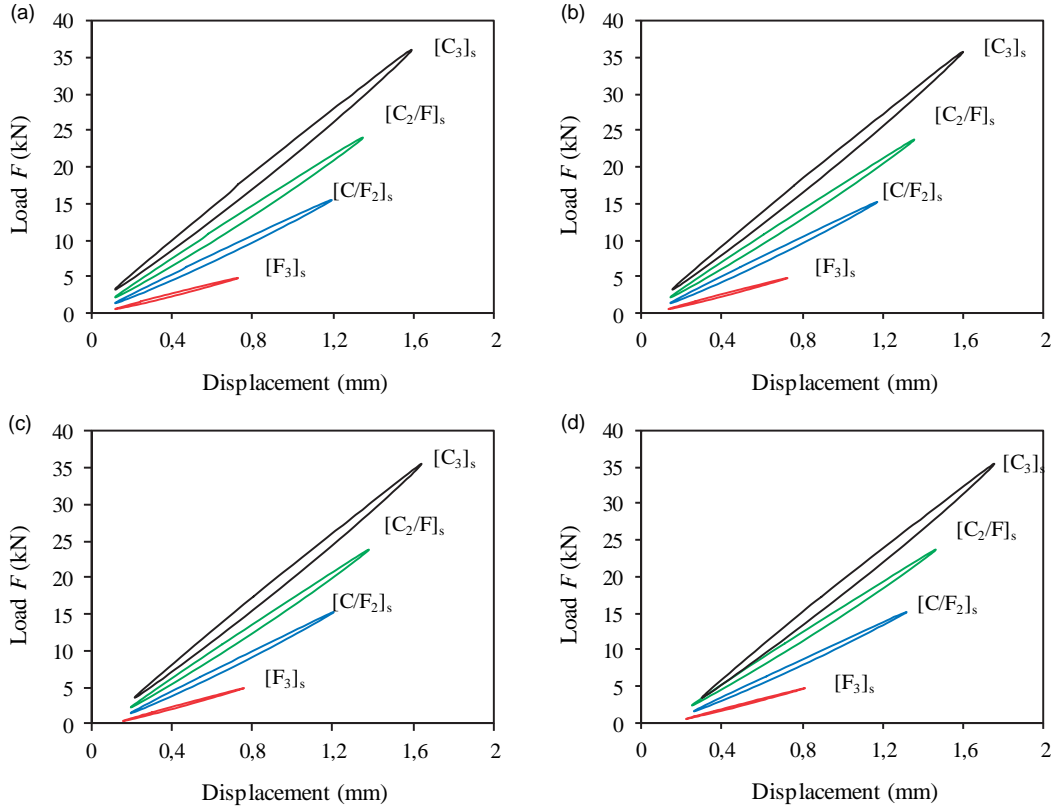


**Figure 8.** Hysteresis curves at  $r = 0.65$  for laminates with external carbon layers at: (a)  $10^0$  cycles, (b)  $10^1$  cycles, (c)  $10^2$  cycles and (d)  $10^3$  cycles.

### Energy dissipation and damping ratio

The area enclosed by the hysteresis loop represents the dissipated energy  $E_d$  as shown in Figure 10. The dissipated energy  $E_d$  can be calculated by integrating the area of the hysteresis loop<sup>21,37</sup> as:

$$E_d = \int_{d_{\min}}^{d_{\max}} F d\delta \quad (1)$$

Where  $d_{\min}$  and  $d_{\max}$  are the minimum and maximum displacements during cyclic loading, respectively. Otherwise, this energy dissipated per cycle is calculated numerically using a simple trapezoidal sum of area. In addition, the potential energy  $E_p$  which is the area under the loading part  $f(d)$  can be calculated by the same method (Figure 10). For each cycle,  $E_d$  and  $E_p$

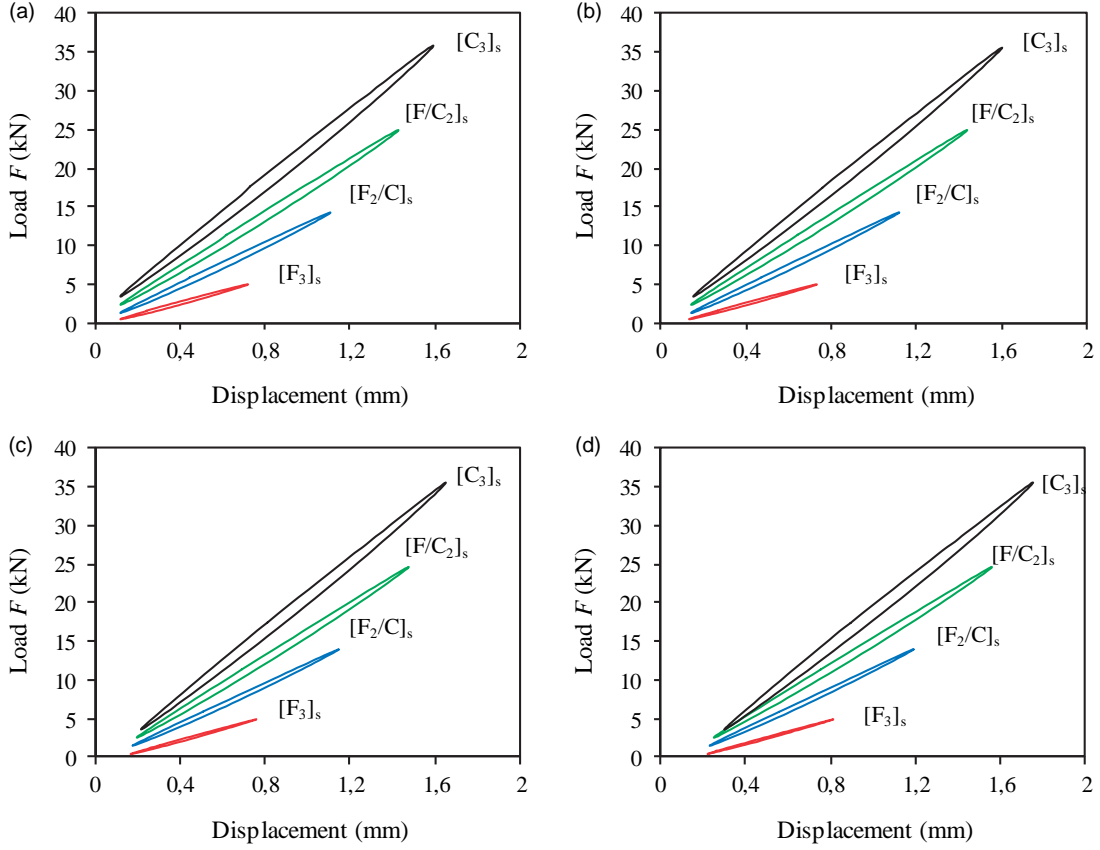


**Figure 9.** Hysteresis curves at  $r = 0.65$  for laminates with internal carbon layers at: (a)  $10^0$  cycles, (b)  $10^1$  cycles, (c)  $10^2$  cycles and (d)  $10^3$  cycles.

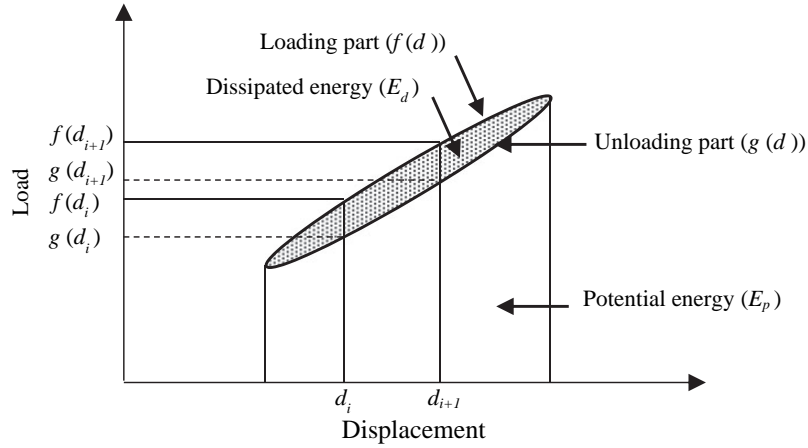


**Figure 10.** Potential energy ( $E_p$ ) and dissipated energy ( $E_d$ ).

are given by:<sup>38,39</sup>

$$E_d = \frac{1}{2} \sum_{i=1}^n (d_{i+1} - d_i) \{ [f(d_{i+1}) + f(d_i)] - [g(d_{i+1}) + g(d_i)] \} \quad (2)$$

$$E_p = \frac{1}{2} \sum_{i=1}^n (d_{i+1} - d_i) [f(d_{i+1}) + f(d_i)] \quad (3)$$

Figure 11 gives a typical result of the dissipated energy as a function of the number of cycles  $N$ , for

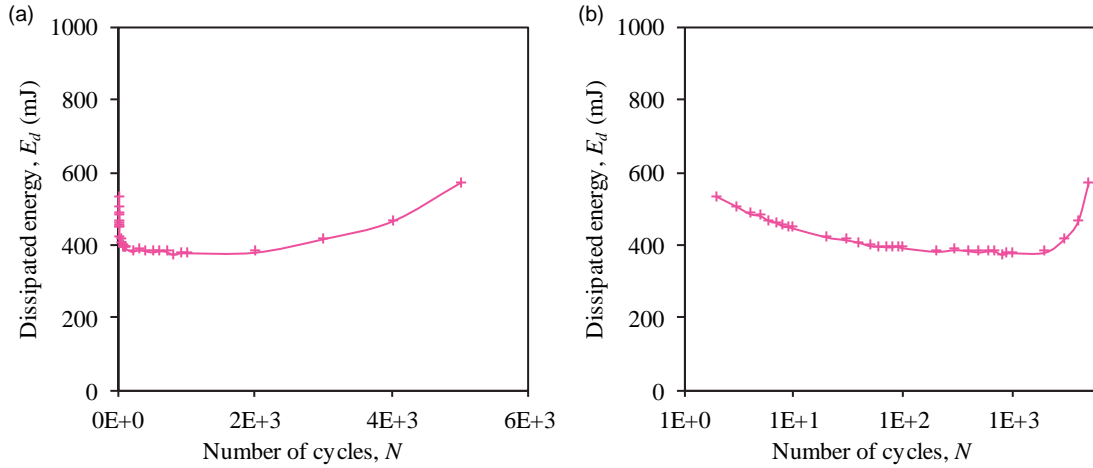


**Figure 11.** A typical curve of the dissipated energy ( $E_d$ ) as a function of the cycle number ( $N$ ): (a) linear scale and (b) semi-logarithmic scale.

the  $[C_3]_s$  laminate with a loading level  $r=0.6$  in both linear and semi-logarithmic scales. The typical curve presented show that it is possible to identify three distinct phases in the evolution of the dissipated energy. The first phase presents a rapid decrease after a few cycles. This phenomenon is often attributed to the initiation of damage mechanisms.<sup>21</sup> Followed by a steady phase, where the energy dissipated is not dependent on the increasing numbers of cycles. This fact can be attributed to the propagation of damage. In the final cycles, we observe a slight increase in the value of the dissipated energy. It can be attributed to the global increase of the damage mechanisms. This evolution in three distinct phases was found by many researchers such as Naderi et al.<sup>40</sup> Thus, the reason can be attributed to the appearance of different damage modes from one phase to the other one. For instance, in transition from phase II to phase III, the dominant damage mechanism changes from matrix cracking and delamination to a more severe matrix cracking and delamination as well as fiber breakage.

Damping ratio or loss factor which depends on the energy dissipated, it is recommended in the evaluation of damage processes in composite materials because it is more sensible than stiffness.<sup>38,39</sup> The loss factor is the ratio of the energy dissipated per cycle  $E_d$  to the potential energy stored per cycle  $E_p$ . The damping factor is calculated as:

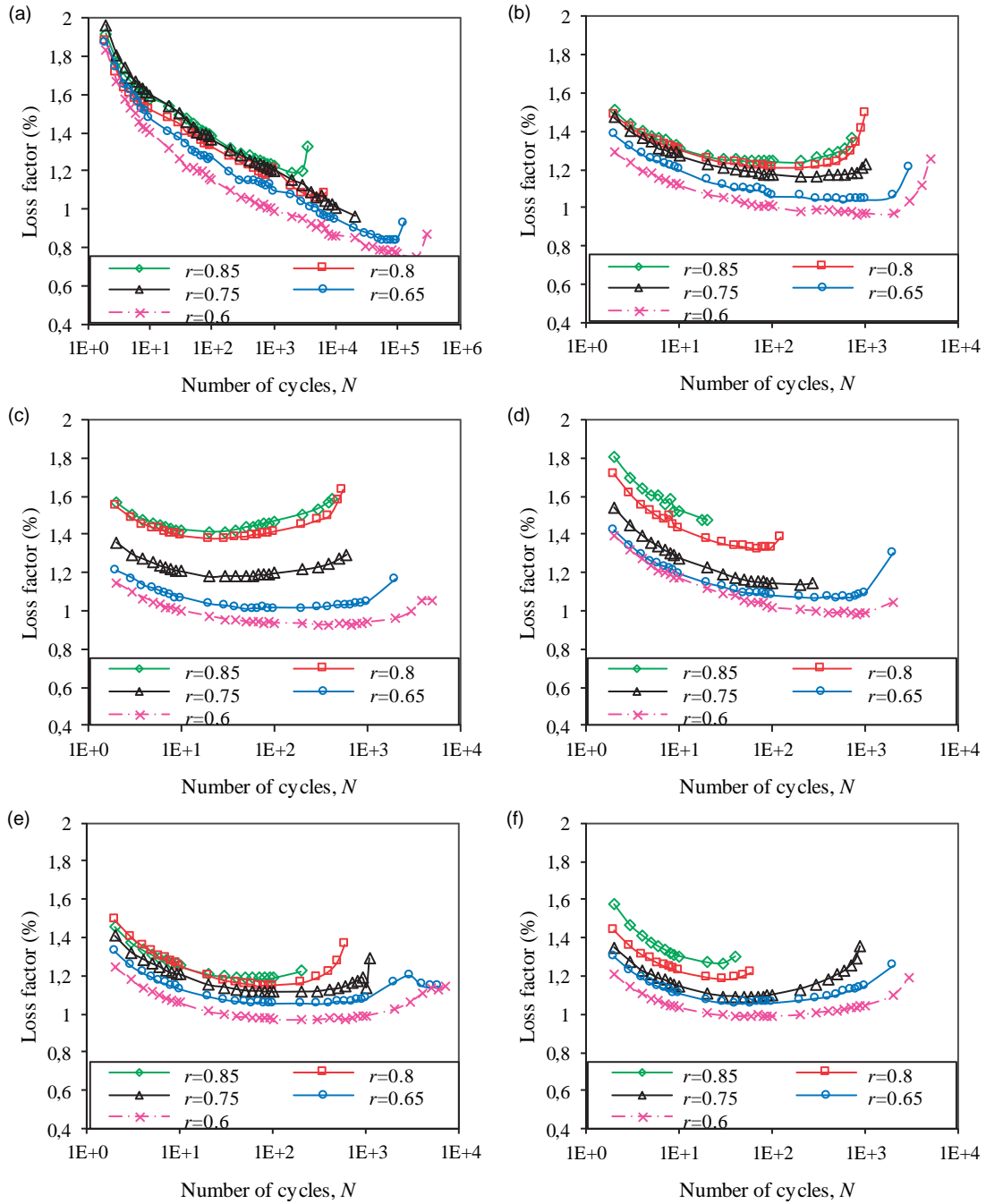
$$\eta = \frac{E_d}{2\pi E_p} \quad (4)$$

Figure 12 illustrates the loss factor as a function of the number of cycles at various applied stress levels ( $r = 0.6, 0.65, 0.75, 0.8$  and  $0.85$ ) for the non-hybrid and hybrid composites using a semi-logarithmic scale.

As shown in Figure 12, the evolution of the loss factor takes place in the three phases identified for all loading levels which is quite similar to the evolution of the dissipated energy.

For the high applied stress level  $r=0.85$ , presented with the green color, the slight increase just before failure in the loss factor is shown in the most of figures, for example in Figure 12(a) is very clear. In addition, for any stacking sequences, it can be seen that the loss factor increases with the increase of the loading level. For instance, the value of the loss factor increases from 1.4% at  $r=0.6$  to an average of 1.6% at  $r=0.85$  for flax laminates and from 1% at  $r=0.6$  to a value around 1.3% at  $r=0.85$  for carbon laminates after 10 cycles. According to Hwang and Gibson,<sup>41</sup> the damping mechanisms are resulting from the viscoelastic nature of fibers and/or matrix, the Coulomb friction damping due to unbounded regions between fiber/fiber or fiber/matrix, the energy dissipation occurring at damage mechanisms and the potential of the applied load. In fact, the differences obtained for each material for the different loading level can be justified by the increase of the dissipated energy caused by the intensity of damage.

Figure 13 shows a comparison between loss factors according to the flax fiber volume fraction for the different stacking sequences at different number of cycles ( $10^0, 10^1, 10^2$  and  $10^3$ ). The damping coefficients of flax fiber laminates are slightly higher than those of carbon fiber laminates. These differences in damping properties between carbon and flax composites can be due to the micro crack at the fiber/matrix interface and to the interface between fibers. Also, it can be attributed to the complex bio-based composite structure due to the viscoelasticity, the architecture and the aspect ratio of flax fiber. According to Duc et al.,<sup>13</sup> the structure of flax fiber raises the dissipation of energy through the



**Figure 12.** Loss factor versus the number of cycles ( $N$ ) at different loading level applied ( $r$ ) and for the different stacking sequences: (a)  $[F_3]_s$ , (b)  $[F_2/C]_s$ , (c)  $[F/C_2]_s$ , (d)  $[C/F_2]_s$ , (e)  $[C_2/F]_s$  and (f)  $[C_3]_s$ .

phenomena of the intra-cell wall friction between cellulose microfibrils and hemicellulose-lignin matrix in each cell wall and the phenomena of inter-cell wall friction between cell walls.

As shown in Figure 13, a comparison between loss factors of hybrid composites with different stacking sequences at same fiber volume fraction for different number of cycles, is carried out. Therefore, the

damping properties are greatly influenced by the position of the flax fiber layers. The results show that the loss factor of composite laminates with internal flax layers is higher than that of composite laminates with external flax layers. In fact, damping of  $[C/F_2]_s$  and  $[C_2/F]_s$  is higher than that of  $[F_2/C]_s$  and  $[F/C_2]_s$ , respectively. For instance,  $[C/F_2]_s$  has a damping coefficient 1.16% higher than that of  $[F_2/C]_s$  by 10% at the cycle

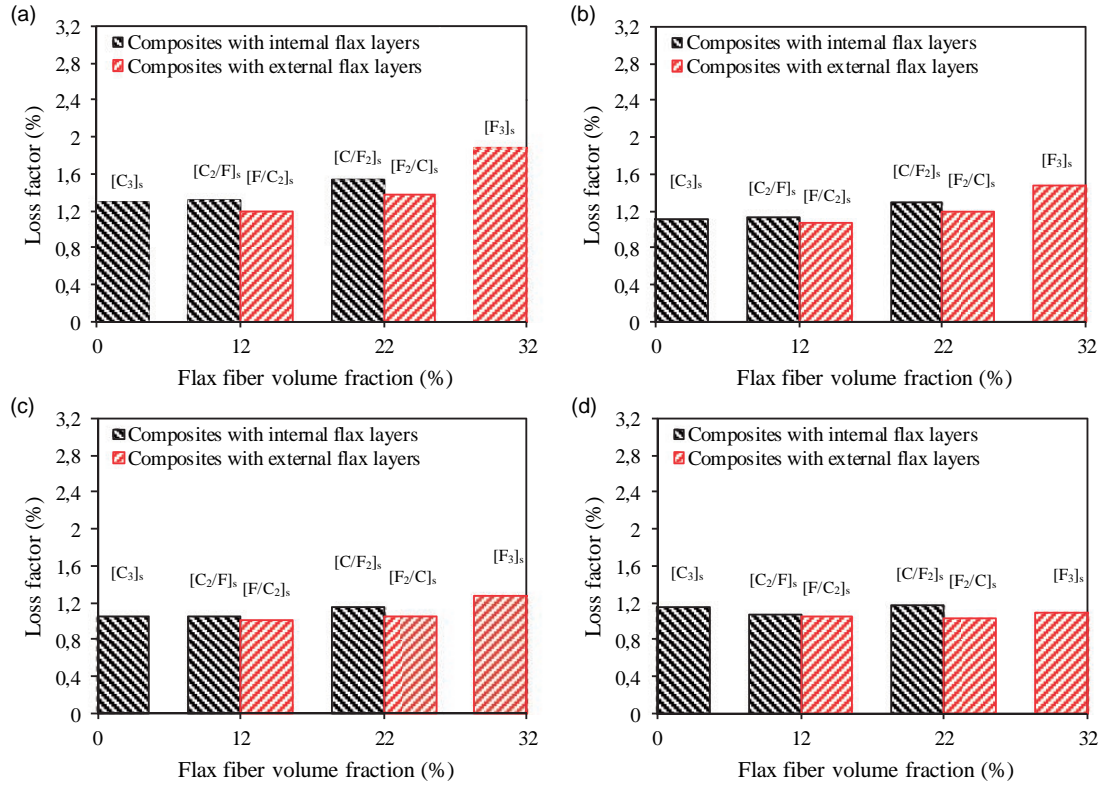


**Figure 13.** Comparison of the loss factor as a function of the flax fiber volume fraction at  $r = 0.65$  for all laminates at cycles number: (a)  $10^0$  cycles, (b)  $10^1$  cycles, (c)  $10^2$  cycles and (d)  $10^3$  cycles.

$10^2$ . As consequence, the damping of the structure is dominated by the internal layers and can be attributed to the friction between internal flax layers.

### S-N curves

The evaluation of the Wohler S-N curves is an important feature of the fatigue behavior of materials. The number of cycles to failure ( $N_r$ ) that express the fatigue life of the different materials were determined from tests at different loading levels (% of respective UTS). A gradual decline in fatigue strength with the increase of the number of fatigue cycles is observed. Wohler's law was used to predict the life of test specimens under fatigue tensile test with imposed load. The mean number of cycles to failure  $N_r^m$  is determined for each stress level and then the endurance curve is plotted using the  $N_r^m$  value obtained at each level. As illustrated in Figure 14, after plotting Wohler stress-life (S-N) diagrams, logarithmic-law regression equations (equation (5)) were determined for each material,

$$\sigma_{\max} = A - B \ln(N_r^m) \quad (5)$$

where  $\sigma_{\max}$  is the maximum (absolute) stress applied (MPa), A and B are intrinsic constants that depend

on the type of material; A is the static ultimate strength of the material for a single cycle, and B is the material fatigue strength coefficient. Equation (5) yields a linear S-N curve on a log plot. Table 3 presents the identified material fatigue parameters (A and B) based on equation (5) and the regression coefficient  $R^2$  of the Wohler curve for each material. All the regression coefficients  $R^2$  are close to 1 ( $R^2 > 0.95$ ), which indicates that the linear relationship used fits well to the experimental fatigue data points.

Subsequently, a comparison of the Wohler S-N curves for the different composite materials was presented in Figure 15. The curves presented reveal that  $[C_3]_s$  specimens exhibit a great resistance to fatigue loading. This result is consistent with the highest static ultimate strength of carbon fiber composites. It can be concluded from this figure that the fatigue resistance of the laminates appears to correlate with their ultimate tensile stress UTS (Table 3). In fact, when the carbon fiber volume fraction increases, the UTS increases and then the fatigue resistance increases. Moreover, the material fatigue strength coefficient B is a very useful parameter. A higher value of B implies a steeper slope of the S-N curve and thus a rapid fatigue strength degradation for every decade of cycles. The slope of the  $[C_3]_s$  curve is steeper

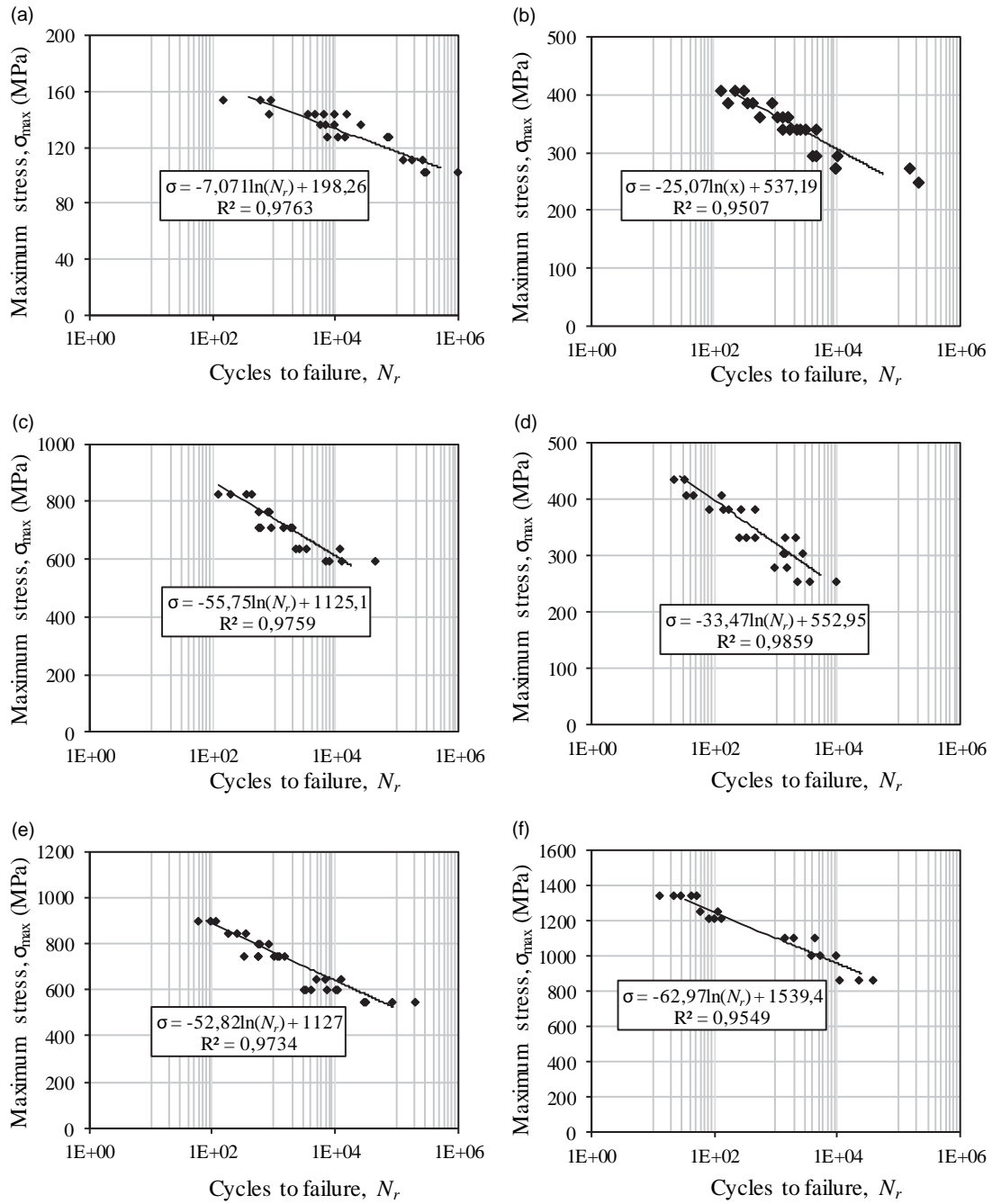


**Figure 14.** Wohler S-N curves for different stacking sequences: (a)  $[F_3]_s$ , (b)  $[F_2/C]_s$ , (c)  $[F/C_2]_s$ , (d)  $[C/F_2]_s$ , (e)  $[C_2/F]_s$  and (f)  $[C_3]_s$ .

**Table 3.** Fatigue properties of the different stacking sequences.

	$[F_3]_s$	$[F_2/C]_s$	$[F/C_2]_s$	$[C/F_2]_s$	$[C_2/F]_s$	$[C_3]_s$
Theoretical ultimate strength A	198.26	537.19	1125	552.95	1127	1539.4
Fatigue strength coefficient B	7.07	25.07	55.75	33.47	52.82	62.97
Regression coefficient $R^2$	0.9763	0.9507	0.9759	0.9859	0.9734	0.9549

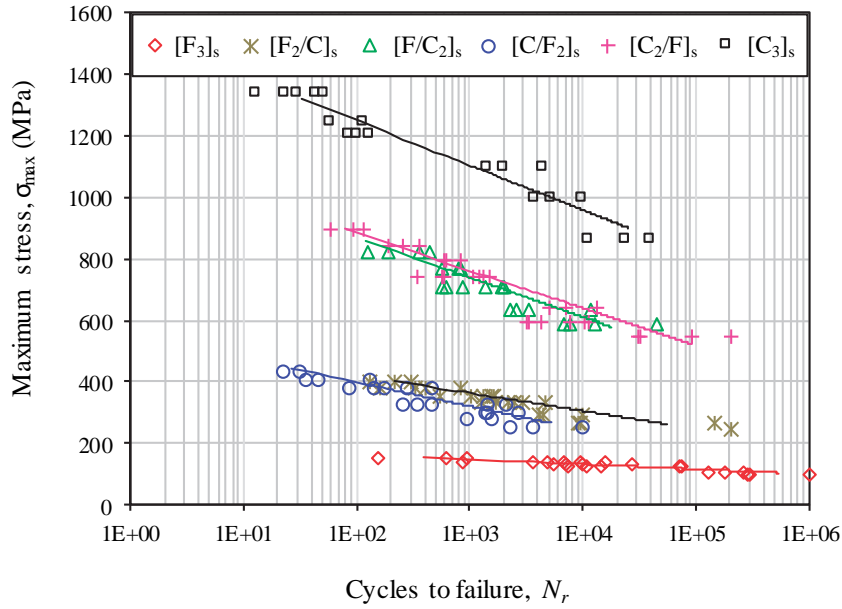


**Figure 15.** Wohler S-N diagram comparing the fatigue performance of the different stacking sequences.

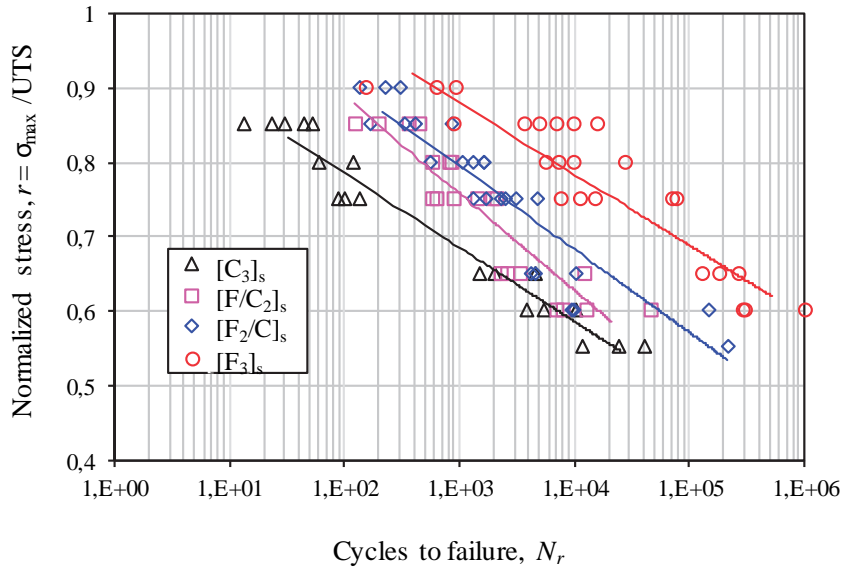


**Figure 16.** Normalized Wohler S-N diagram comparing the fatigue performance of  $[F_3]_s$ ,  $[F_2/C]_s$ ,  $[F/C_2]_s$  and  $[C_3]_s$ .

( $B = 62.9$ ) than that of  $[F_3]_s$  ( $B = 7$ ), implying an important decrease of the stress level according the fatigue life. In addition, the slope of the different materials increases with the increase of the carbon fiber volume fraction. These observations confirm that the ultimate stress UTS can correlates with the fatigue resistance, indeed the fatigue strength coefficient  $B$  can be used as an indicator for prediction of the lifetime fatigue performance. Although the interface between the flax fiber and the epoxy matrix is weak due to poor adhesion of the hydrophilic plant fibers to the hydrophobic

matrix,<sup>42-44</sup> the accumulation rate of the damage in  $[F_3]_s$  laminates is slower than in  $[C_3]_s$  laminates. This behavior could be justified by the straightening of the microfibrils. In fact, the progressive reorientation of cellulose microfibrils in vegetal fibers towards the direction of loading is the most possible explanation for this observation.<sup>24,25,45</sup>

From the Table 3 and the S-N diagram in Figure 15, it is observed that the fatigue strength coefficients  $B$  are very similar for the hybrid laminates with same volume fraction of fibers but with different position of layers.

For instance,  $[F/C_2]_s$  and  $[C_2/F]_s$  composites have similar rates of fatigue strength degradation. This result indicates that the resulting gradual fatigue strength and the fatigue failure mechanism are independent to the position of layers.

Wohler S-N curves of  $[F_3]_s$ ,  $[F_2/C]_s$ ,  $[F/C_2]_s$  and  $[C_3]_s$  laminates are presented in Figure 16 in normalized form ( $r = \sigma_{max}/UTS$ ) according to the number of cycle to failure. The normalized S-N diagram readily enables the comparison of the endurance performance of the different materials. From Figure 16, it is immediately clear that  $[F_3]_s$  laminate seems to have the best endurance performance and  $[C_3]_s$  laminate seems to have the lowest. In fact, while normalizing the S-N curve, Figure 16 suggests better performance when adding the flax fibers. However, in real application Figure 15 is to be followed which suggest that adding flax significantly reduces the fatigue strength of the carbon fiber composite which limiting the application of these composites to situations with minimal applied stress.

## Conclusion

The present work focuses on the experimental analysis of the static and cyclic tensile properties of non-hybrid and hybrid composite materials made of thermoset epoxy resin reinforced with flax and carbon fibers. The carbon laminates, the flax laminates and the different stacking sequences of hybrid laminates were manufactured by manual lay-up process. At first, quasi-static tensile tests were performed to determine the ultimate properties of the different stacking sequences. The non-hybrid and hybrid laminates were tested under cyclic fatigue tests for different applied stress levels in order to analyze their behavior for the different loading levels. The tests were performed at applied stress ratio  $R$  of 0.1. For each laminate, the stiffness depends on the applied stress level. The energy dissipated per cycle increases with the applied loading level. In addition, for each applied loading level, it increases near the end of the fatigue lifetime as a result of the increase in the area enclosed by the hysteresis loops. A comparison was made between the different composite materials studied under the fatigue tensile tests up to  $10^3$  cycles. The evolution of the loss factor with the number of cycles during fatigue cycles was also studied. It reveals interesting damping properties for hybrid laminates. Also we find that flax fibers tend to reduce the fatigue strength. It was also shown from the Wohler diagrams that the fatigue properties increase with the increase of carbon fiber content. That's why composites having higher static strength exhibited better fatigue resistance. One can conclude that this hybrid material would be suitable for some semi-structural applications currently using carbon fiber composite structures and

subjected to fatigue loading. For future works, additional experimental tests involving non-destructive methods such as the acoustic emission technique, could probably help to determine the correlation between damage evolution and loss factor evolution.


## Declaration of Conflicting Interests

The author(s) declared no potential conflicts of interest with respect to the research, authorship, and/or publication of this article.

## Funding

The author(s) received no financial support for the research, authorship, and/or publication of this article.

## ORCID iD

Mariem Ben Ameer  <https://orcid.org/0000-0001-6080-341X>

## References

1. Pickering KL, Efendy MGA and Le TM. A review of recent developments in natural fibre composites and their mechanical performance. *Compos Part Appl Sci Manuf* 2016; 83: 98–112.
2. Faruk O, Bledzki AK, Fink HP, et al. Biocomposites reinforced with natural fibers: 2000–2010. *Prog Polym Sci* 2012; 37: 1552–1596.
3. Stamboulis A, Baillie CA and Peijs T. Effects of environmental conditions on mechanical and physical properties of flax fibers. *Compos Part Appl Sci Manuf* 2001; 32: 1105–1115.
4. Wambua P, Ivens J and Verpoest I. Natural fibres: can they replace glass in fibre reinforced plastics? *Compos Sci Technol* 2003; 63: 1259–1264.
5. Al-Oqla FM and Sapuan SM. Natural fiber reinforced polymer composites in industrial applications: feasibility of date palm fibers for sustainable automotive industry. *J Clean Prod* 2014; 66: 347–354.
6. Oksman K. High quality flax fibre composites manufactured by the resin transfer moulding process. *J Reinf Plast Compos* 2001; 20: 621–627.
7. Van de Weyenberg I, Ivens J, De Coster A, et al. Influence of processing and chemical treatment of flax fibres on their composites. *Compos Sci Technol* 2003; 63: 1241–1246.
8. Yan L, Chow N and Jayaraman K. Flax fibre and its composites – a review. *Compos Part B Eng* 2014; 56: 296–317.
9. Monti A, El Mahi A, Jendli Z, et al. Mechanical behavior and damage mechanisms analysis of a flax-fibre reinforced composite by acoustic emission. *Compos Part Appl Sci Manuf* 2016; 90: 100–110.
10. Haggui M, El Mahi A, Jendli Z, et al. Static and fatigue characterization of flax fiber reinforced thermoplastic composites by acoustic emission. *Appl Acoust* 9; 147: 100–110.



11. Hughes M, Carpenter J and Hill C. Deformation and fracture behavior of flax fibre reinforced thermosetting polymer matrix composites. *J Mater Sci* 2007; 42: 2499–2511.
12. Monti A, El Mahi A, Jendli Z, et al. Experimental and finite elements analysis of the vibration behavior of a bio-based composite sandwich beam. *Compos Part B Eng* 2017; 110: 466–475.
13. Duc F, Bourban PE, Plummer CJG, et al. Damping of thermoset and thermoplastic flax fibre composites. *Compos. Part Appl Sci Manuf* 2014; 64: 115–123.
14. Dhakal HN, Zhang ZY, Guthrie R, et al. Development of flax/carbon fibre hybrid composites for enhanced properties. *Carbohydr Polym* 2013; 96: 1–8. vol.
15. de Moura MFSF, Fernandes R, Silva FGA, et al. Mode II fracture characterization of a hybrid Cork/carbon-epoxy laminate. *Compos Part B Eng* 2015; 76: 44–51.
16. Atiqah A, Maleque MA, Jawaid M, et al. Development of kenaf-glass reinforced unsaturated polyester hybrid composite for structural applications. *Compos Part B Eng* 2014; 56: 68–73.
17. Assarar M, Zouari W, Sabhi H, et al. Evaluation of the damping of hybrid carbon–flax reinforced composites. *Compos Struct* 2015; 132: 148–154.
18. Ben Ameer M, El Mahi A, Rebiere JL, et al. Damping analysis of unidirectional carbon/flax fiber hybrid composites. *Int J Appl Mechanics* 2018; 10: 1850050.
19. Flynn J, Amiri A and Ulven C. Hybridized carbon and flax fiber composites for tailored performance. *Mater Des* 2016; 102: 21–29.
20. Fiore V, Valenza A and Di Bella G. Mechanical behavior of carbon/flax hybrid composites for structural applications. *J Compos Mater* 2012; 46: 2089–2096.
21. Belaadi A, Bezazi A, Bouchak M, et al. Tensile static and fatigue behavior of sisal fibres. *Mater Des* 2013; 46: 76–83.
22. de Andrade Silva F, Chawla N and de Toledo Filho RD. An experimental investigation of the fatigue behavior of sisal fibers. *Mater Sci Eng A* 2009; 516: 90–95.
23. Towo AN and Ansell MP. Fatigue of sisal fibre reinforced composites: constant-life diagrams and hysteresis loop capture. *Compos Sci Technol* 2008; 68: 915–924.
24. Liang S, Gning PB and Guillaumat L. A comparative study of fatigue behaviour of flax/epoxy and glass/epoxy composites. *Compos Sci Technol* 2012; 72: 535–543.
25. Shah DU, Schubel PJ, Clifford MJ, et al. Fatigue life evaluation of aligned plant fibre composites through S–N curves and constant-life diagrams. *Compos Sci Technol* 2013; 74: 139–149.
26. El Sawi I, Fawaz Z, Zitoune R, et al. An investigation of the damage mechanisms and fatigue life diagrams of flax fiber-reinforced polymer laminates. *J Mater Sci* 2014; 49: 2338–2346.
27. Mahboob Z and Bougherara H. Fatigue of flax-epoxy and other plant fibre composites: critical review and analysis. *Compos Part Appl Sci Manuf* 2018; 109: 440–462.
28. Gassan J. A study of fibre and interface parameters affecting the fatigue behaviour of natural fibre composites. *Compos Part A* 2002; 33: 369–374.
29. Bensadoun F, Vallons KAM, Lessard LB, et al. Fatigue behaviour assessment of flax–epoxy composites. *Compos Part Appl Sci Manuf* 2016; 82: 253–266.
30. Zhang Z and Hartwig G. Relation of damping and fatigue damage of unidirectional fibre composites. *Int J Fatigue* 2002; 24: 713–718.
31. Khalfallah M, Abbès B, Abbès F, et al. Innovative flax tapes reinforced acrodur biocomposites: a new alternative for automotive applications. *Mater Des* 2014; 64: 116–126.
32. Baley C, Le Duigou A, Bourmaud A, et al. Influence of drying on the mechanical behaviour of flax fibres and their unidirectional composites. *Compos Part Appl Sci Manuf* 2012; 43: 1226–1233.
33. Malloum A, El Mahi A and Idriss M. The effects of water ageing on the tensile static and fatigue behaviors of greenepoxy–flax fiber composites. *J Compos Mater* 2019; 53: 2927–2913.
34. ASTM D30309/D3039M-14: Standard test method for tensile properties of polymer matrix composite.
35. Bezazi A, El Mahi A, Berthelot JM, et al. Investigation of Cross-Ply laminates behaviour in three point bending tests. Part II: cyclic fatigue tests. *Mater Sci (Medžiagotyra)* 2003; 9: 1392–1320.
36. Bezazi A, El Mahi A, Berthelot JM, et al. Flexural fatigue behavior of cross-ply laminates: an experimental approach. *Strength Mater* 2003; 35: 149–183.
37. Farooq MK. *Comportement mécanique des composites sandwichs en statique et fatigue cyclique*. PhD dissertation, Le Mans Université, France, 2003.
38. Idriss M, El Mahi A, Assarar M, et al. Damping analysis in cyclic fatigue loading of sandwich beams with debonding. *Compos Part B Eng* 2013; 44: 597–603.
39. Ben Ammar I, Karra C, El Mahi A, et al. Mechanical behavior and acoustic emission technique for detecting damage in sandwich structures. *Appl Acoust* 2014; 86: 106–117.
40. Naderi M, Kahirdeh A and Khonsari MM. Dissipated thermal energy and damage evolution of glass/epoxy using infrared thermography and acoustic emission. *Compos: Part B* 2012; 43: 1613–1620.
41. Hwang SJ and Gibson RF. The use of strain energy-based finite element techniques in the analysis of various aspects of damping of composite materials and structures. *J Compos Mater* 1992; 26: 2585–2605.
42. Kalia S, Kaith BS and Kaur I. Pretreatments of natural fibers and their application as reinforcing material in polymer composites – a review. *Polym Eng Sci* 2009; 49: 1253–1272.
43. Mwaikambo L and Ansell MP. Chemical modification of hemp, sisal, jute and kapok fibers by alkalization. *J Appl Polym Sci* 2002; 84: 2222–2234.
44. John M and Anandjiwala RD. Recent developments in chemical modification and characterization of natural fiber-reinforced composites. *Polym Compos* 2008; 29: 187–207.
45. Spatz H, Kohler L and Niklas KJ. Mechanical behaviour of plant tissues: composite materials or structures? *J Exp Biol* 1999; 202: 3269–3272.